Constitutive Activation of the Calcium Sensor STIM1 Causes Tubular-Aggregate Myopathy

Johann Böhm, Frédéric Chevessier, André Maues de Paula, Catherine Koch, Shahram Attarian, Claire Feger, Daniel Hantaï, Pascal Laforêt, Karima Ghorab, Jean-Michel Vallat, et al.

Constitutive Activation of the Calcium Sensor STIM1 Causes Tubular-Aggregate Myopathy

Johann Böhm,[1,2,3,4,5] Frédéric Chevessier,[6,18,19] André Maues De Paula,[7,8,9,18] Catherine Koch,[1,2,3,4,5] Shahram Attarian,[10] Claire Feger,[1,2,3,4,5] Daniel Hantaï,[6,11] Pascal Laforêt,[6] Karima Ghorab,[12] Jean-Michel Vallat,[12] Michel Fardeau,[6,13] Dominique Figarella-Branger,[9] Jean Pouget,[10] Norma B. Romero,[6,13,14] Marc Koch,[2,3,4,15] Claudine Ebel,[2,3,4,16] Nicolas Levy,[7,8,17] Martin Krahn,[7,8,17] Bruno Eymard,[6] Marc Bartoli,[7,8,17] and Jocelyn Laporte[1,2,3,4,5,*]

Tubular aggregates are regular arrays of membrane tubules accumulating in muscle with age. They are found as secondary features in several muscle disorders, including alcohol- and drug-induced myopathies, exercise-induced cramps, and inherited myasthenia, but also exist as a pure genetic form characterized by slowly progressive muscle weakness. We identified dominant *STIM1* mutations as a genetic cause of tubular-aggregate myopathy (TAM). Stromal interaction molecule 1 (STIM1) is the main Ca^{2+} sensor in the endoplasmic reticulum, and all mutations were found in the highly conserved intraluminal Ca^{2+}-binding EF hands. Ca^{2+} stores are refilled through a process called store-operated Ca^{2+} entry (SOCE). Upon Ca^{2+}-store depletion, wild-type STIM1 oligomerizes and thereby triggers extracellular Ca^{2+} entry. In contrast, the missense mutations found in our four TAM-affected families induced constitutive STIM1 clustering, indicating that Ca^{2+} sensing was impaired. By monitoring the calcium response of TAM myoblasts to SOCE, we found a significantly higher basal Ca^{2+} level in TAM cells and a dysregulation of intracellular Ca^{2+} homeostasis. Because recessive *STIM1* loss-of-function mutations were associated with immunodeficiency, we conclude that the tissue-specific impact of STIM1 loss or constitutive activation is different and that a tight regulation of STIM1-dependent SOCE is fundamental for normal skeletal-muscle structure and function.

Ca^{2+} is a major regulatory and signaling molecule in skeletal muscle; therefore, the cellular Ca^{2+} dynamics need to be tightly regulated. Intracellular Ca^{2+} is mainly stored in the sarcoplasmic reticulum (SR) and, upon stimulation, is released to the cytoplasm, where it triggers muscle contraction and acts as a second messenger controlling growth and differentiation. Ca^{2+} stores are refilled through store-operated Ca^{2+} entry (SOCE). Stromal interaction molecule 1 (STIM1) is the main Ca^{2+} sensor on the endoplasmic reticulum (ER). It contains an intraluminal region with two EF hands and a sterile α-motif domain (SAM), a single transmembrane domain, and a cytosolic part interacting with other proteins.[1,2] The EF hands sense and bind Ca^{2+}, and in the bound state, the EF hands and the SAM domain are in steric proximity. When Ca^{2+} is unbound as a result of store depletion, STIM1 unfolds and oligomerizes through its SAM domains.[2,3] The oligomerization activates Ca^{2+}-release-activated Ca^{2+} channels (CRACs) by direct binding to ORAI1 and thereby triggers extracellular Ca^{2+} entry.[1,4–7]

In this paper, we describe four families affected by dominant tubular-aggregate myopathy (TAM [MIM 160565]), which is characterized by regular arrays of membrane tubules on muscle biopsies without additional histopathological hallmarks (Table 1 and Table S1, available online). Apart from this "pure" form, tubular aggregates can also be found as secondary features in a variety of muscle disorders, including alcohol- and drug-induced myopathies, exercise-induced cramps or muscle weakness, and inherited myopathies and myasthenia.[8,9] In our TAM-affected families, disease onset was during childhood (individuals II.1 and II.2 from family 1, II.10 from family 2, and I.2 and II.2 from family 3), adolescence (I.1 from family 1 and II.2 from family 2), or early adulthood (III.1 from family 2), and all presented predominantly with mild and slowly progressive lower-limb muscle weakness.

[1]Département de Médecine Translationelle et Neurogénétique, Institut de Génétique et de Biologie Moléculaire et Cellulaire, 67404 Illkirch, France; [2]Unité 964, Institut National de la Santé et de la Recherche Médicale, 67404 Illkirch, France; [3]Unité Mixte de Recherche 7104, Centre National de la Recherche Scientifique, 67404 Illkirch, France; [4]Université de Strasbourg, 67404 Illkirch, France; [5]Chaire de Génétique Humaine, Collège de France, 67404 Illkirch, France; [6]Centre de Référence de Pathologie Neuromusculaire Paris Est, Groupe Hospitalier Pitié-Salpêtrière, 75013 Paris, France; [7]Unité Mixte de Recherche S910, Faculté de Médecine de Marseille, Aix-Marseille Université, 13385 Marseille, France; [8]Unité Mixte de Recherche S910, Institut National de la Santé et de la Recherche Médicale, 13385 Marseille, France; [9]Service d'Anatomie Pathologique et Neuropathologie, Hôpital de la Timone, Assistance Publique Hopitaux de Marseille, 13385 Marseille, France; [10]Centre de Référence des Maladies Neuromusculaires et de la Sclérose Latérale Amyotrophique, Hôpital d'Enfants de la Timone, 13385 Marseille, France; [11]Institut National de la Santé et de la Recherche Médicale Unité Mixte de Recherche S975, Centre de Recherche de l'Institut du Cerveau et de la Moëlle, Hôpital Pitié-Salpêtrière, 75013 Paris, France; [12]Département de Neurologie et Centre National de Référence Neuropathies Périphériques Rares, Centre Hospitalier Universitaire de Limoges, 87042 Limoges, France; [13]Unité de Morphologie Neuromusculaire, Institut de Myologie, Groupe Hospitalier Universitaire La Pitié-Salpêtrière, 75013 Paris, France; [14]Université Pierre et Marie Curie (Paris 6) Unité R76, Institut National de la Santé et de la Recherche Médicale Unité Mixte de Recherche 974, and Centre National de la Recherche Scientifique Unité Mixte de Recherche 7215, Institut de Myologie, Groupe Hospitalier Universitaire La Pitié-Salpêtrière, 75013 Paris, France; [15]Centre d'Imagerie, Institut de Génétique et de Biologie Moléculaire et Cellulaire, 67404 Illkirch, France; [16]Plateforme de Cytométrie, Institut de Génétique et de Biologie Moléculaire et Cellulaire, 67404 Illkirch, France; [17]Département de Génétique Médicale, Hôpital d'Enfants de la Timone, Assistance Publique Hopitaux de Marseille, 13385 Marseille, France
[18]These authors contributed equally to this work
[19]Present address: Department of Neuropathology, University Hospital Erlangen, 91054 Erlangen, Germany
*Correspondence: jocelyn@igbmc.fr

Table 1. Molecular, Phenotypic, and Histopathological Data of Individuals with Dominant *STIM1* Mutations

	Family 1			Family 2			Family 3		Family 4		
	I.1	II.1	II.2	II.2	II.10	III.1	I.2	II.2	I.2	II.1	II.2
Gender	female	male	male	female	male	female	male	male	male	male	male
Mutation	c.251A>G	c.251A>G	c.251A>G	c.325C>A	c.325C>A	c.325C>A	c.326A>G	c.326A>G	c.216C>G	c.216C>G	c.216C>G
Predicted protein impact	p.Asp84Gly	p.Asp84Gly	p.Asp84Gly	p.His109Asn	p.His109Asn	p.His109Asn	p.His109Arg	p.His109Arg	p.His72Gln	p.His72Gln	p.His72Gln
Onset	adolescence	childhood	childhood	adolescence	childhood	adulthood	childhood	childhood	asymptomatic	asymptomatic	asymptomatic
Age at last examination (years)	61	54	49	68	51	41	57	33	59	30	24
Muscle weakness	lower limbs proximal	lower limbs proximal, upper limbs mild and diffuse	lower limbs proximal	lower limbs proximal	lower limbs proximal	lower limbs proximal, upper limbs mild and proximal	severe, upper and lower limbs, predominantly proximal	lower limbs proximal, upper limbs mild and proximal	no	no	no
Eye-movement defects	mild upward-gaze paresis	mild upward- and lateral-gaze paresis	upward-gaze paresis	no	no	no	ophthalmoplegia, upward-gaze paresis	ophthalmoplegia, upward-gaze paresis	no	no	no
Contractures	no	heels, wrists, fingers	heels, wrists, fingers	no	knees	heels	severe, neck, elbows, wrists, fingers	neck, heels	no	no	no
CK levels	elevated	8× elevated	4× elevated	4× elevated	5× elevated	7× elevated	5× elevated	12× elevated	5× elevated	27× elevated	9× elevated
Tubular-aggregate classification	ND	in type I and II fibers, VMC and IC	ND	in type I and II fibers, VMC and IC	in type I and II fibers, VMC and IC	mainly in type I fibers, VMC and IC	mainly in type I fibers, VMC and IC	in type I and II fibers, VMC and IC	in type I and II fibers, VMC and IC	in type I and II fibers, VMC and IC	in type I and II fibers, VMC and IC
Specific histological features	ND	fiber size variation, type I fiber predominance	ND	type II fiber atrophy	type II fiber atrophy	type II fiber atrophy	type I fiber predominance, type II fiber atrophy	type I fiber predominance, type II fiber atrophy	fiber size variation, type I fiber predominance, type II fiber atrophy	fiber size variation, type I fiber predominance, type II fiber atrophy	fiber size variation, type I fiber predominance, type II fiber atrophy

The following abbreviations are used: CK, creatine kinase; ND, not determined; VMC, vesicular membrane collection (according to Chevessier et al.[8]); and IC, tubular aggregates with empty or moderately dense flocculent material.

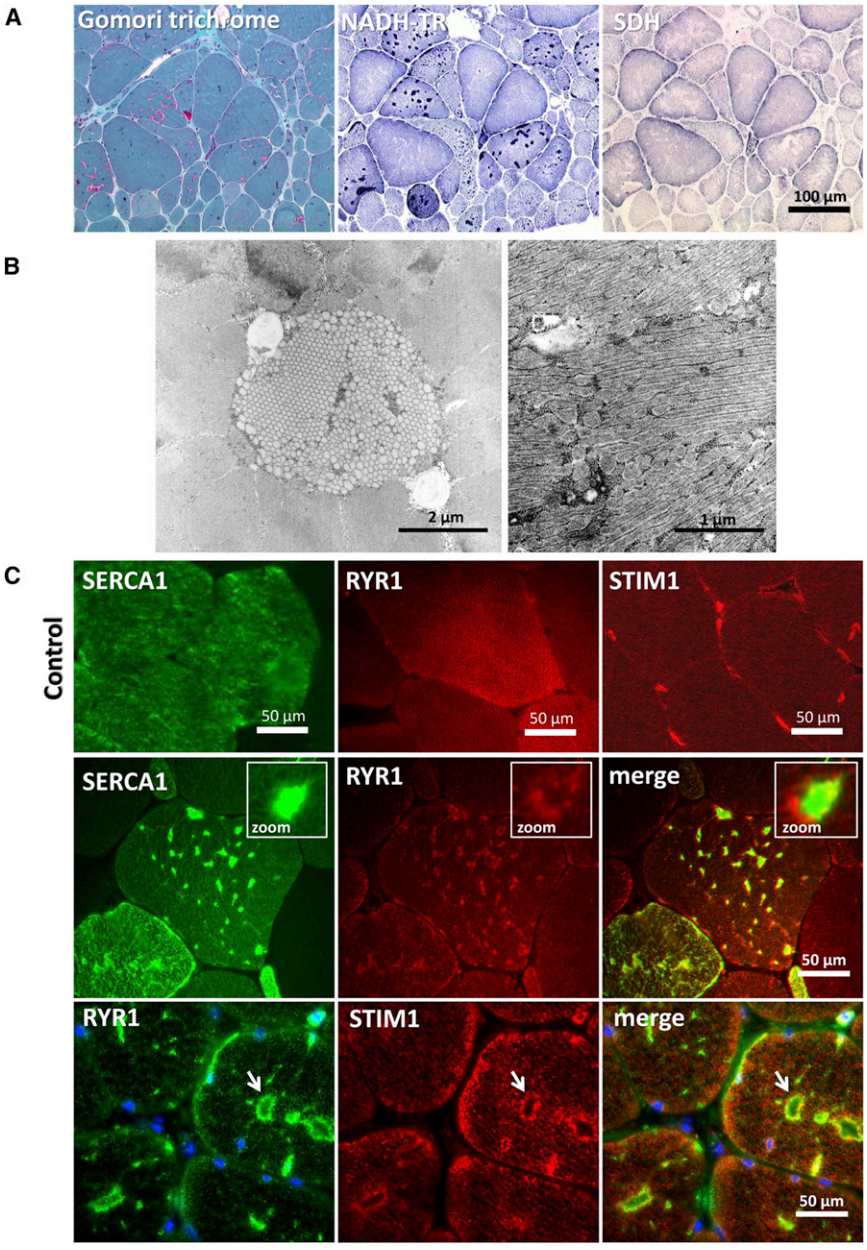

Figure 1. Characterization of Tubular Aggregates in Skeletal Muscle

Histology, immunofluorescence, and electron microscopy of muscle biopsies from affected individuals II.1 (family 1, p.Asp84Gly) and III.1 (family 2, p.His109Asn).

(A) Histological analysis of transverse sections (10 µm) revealed aggregations on modified Gomori trichrome and NADH-TR staining, but not on succinic-dehydrogenase (SDH) staining (II.1, family 1).

(B) Ultrastructural analysis demonstrated prominent tubular aggregation with single- or double-walled membranes on transversal (II.1, family 1) and longitudinal (III.1, family 2) sections.

(C) Immunofluorescence showed colocalization of STIM1 and RYR1 in the periphery of the aggregates, whereas SERCA1 homogeneously labeled the aggregates (II.1, family 1). The upper panel shows muscle sections of a healthy individual.

Ophthalmoparesis without ptosis was mild in family 1 and severe in family 3, and contractures of the elbows, wrist and fingers, heel cords, and neck were reported for both families. Individual II.1 from family 1 had a 1-week-long paresis of the lower limbs at age 9, and III.1 from family 2 had a period of worsening and moderate variability. No cardiac involvement was reported, and breathing was normal except for family 3 member I.2, who required intermittent nocturnal ventilation. At the last medical examination, all affected individuals except I.2 from family 3 were ambulant. The three TAM-affected individuals from family 4 were asymptomatic, although needle electromyography using quantitative analysis of 20 motor unit potentials revealed a slight myopathic pattern in II.1 (Figure S1). This might be related to the specific mutation or to the fact that these persons underwent regular and strong physical training as a part of their military duties. The muscle disorder was detected through routine creatine-kinase (CK) blood tests. CK levels were strongly elevated in affected individuals from all families, and electrophysiological analyses revealed a myopathic pattern in all tested individuals (there was no decrement at testing).

Muscle biopsies of the affected individuals displayed predominantly type II fiber atrophy (Figures S2 and S3); aggregates appeared in red on Gomori trichrome and in dark blue on NADH-TR staining (Figure 1A and Figure S3). The aggregates were absent with succinic-dehydrogenase (SDH) staining, indicating a reticular, but not mitochondrial, origin.[10,11] Ultrastructural analysis demonstrated massive tubular aggregation and single- or double-walled membranes of different diameters (Figure 1B). Tubular aggregates originate from the SR,[8,10,11] but the exact mechanisms leading to their formation in skeletal muscle fibers are elusive.[12] We have previously shown that different proteins involved in the uptake and storage of calcium, such as SERCA1, sarcalumenin, or triadin, are components of the aggregates.[8] Here, we demonstrated by immunohistofluorescence using antibodies against markers of the SR that SERCA1 and triadin strongly label the aggregates, whereas RYR1 and STIM1 localize in their periphery (Figure 1C and Figures S4 and S5). This might be linked to the fact that SERCA1 and triadin localize at the longitudinal SR, whereas RYR1 and STIM1 localize at the junctional SR, suggesting the presence of triads at the periphery of the aggregates as documented

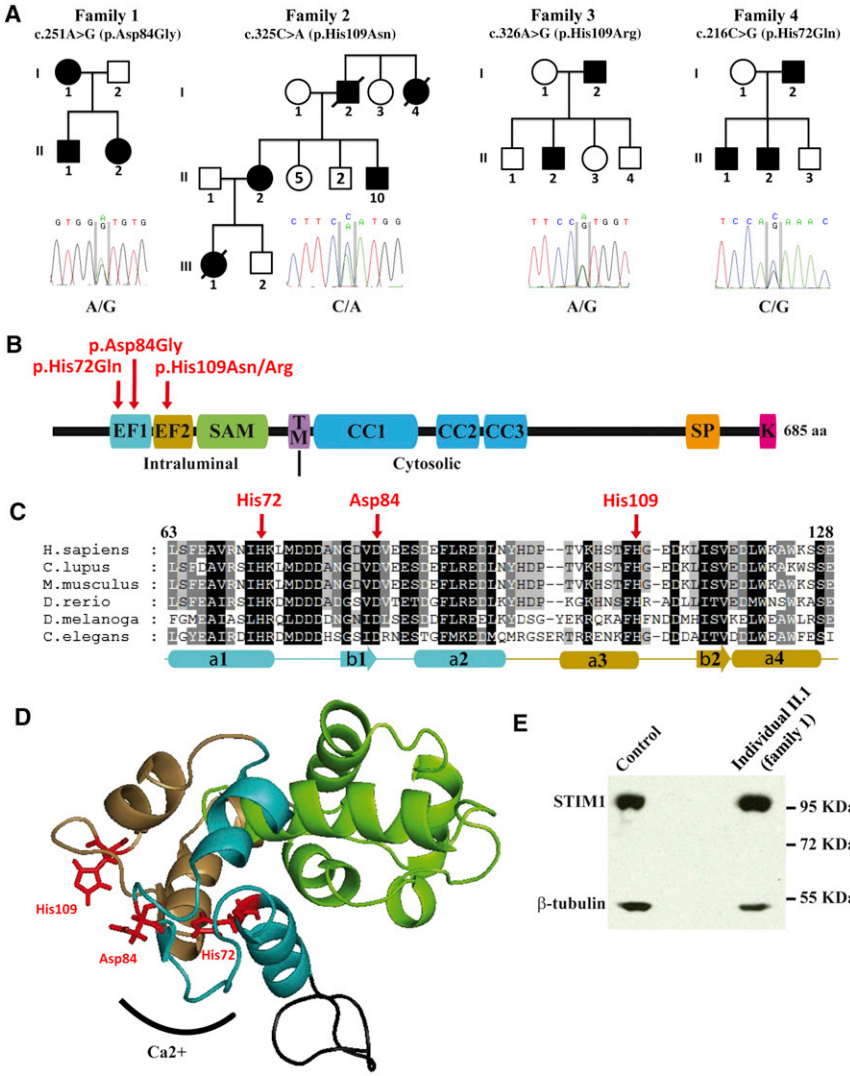

Figure 2. Identification of *STIM1* Mutations in Autosomal-Dominant TAM

(A) Pedigrees indicate dominant inheritance of TAM, and sequence analysis confirmed the segregation of the heterozygous mutations with the disease.

(B) Schematic representation of the STIM1 domains. Arrows indicate the position of the substitutions in the EF-hand domains (amino acids 63–128). The following abbreviations are used: TM , transmembrane domain; CC, coiled-coil domain; SP, serine- and proline-rich domain; and K, polylysine.

(C) Protein-sequence conservation of the STIM1 EF hands. The affected amino acids are highly conserved.

(D) The resolved protein structure demonstrates a close proximity of the affected amino acids to the Ca^{2+}-binding domain.

(E) Immunoblot of endogenous STIM1 in individual II.1 from family 1 and control myoblasts shows a comparable STIM1 level. β-Tubulin was used as a loading control.

by electron microscopy.[8,9] Tubular aggregates were mainly reported in males from recessive families or simplex cases and were most often found only in type II fibers.[12] In contrast, in this study, we describe autosomal-dominant TAM-affected families involving both genders and both types of muscle fibers. This strongly suggests that different genes are implicated in the dominant and recessive TAM forms.

In order to identify the genetic cause of dominant TAM, we performed exome sequencing of all four members of family 1 by using the Agilent SureSelect Human All Exon Kit and the Illumina Genome Analyzer IIx to generate 72 nt single reads. Sample collection was performed with informed consent from the affected individuals according to the declaration of Helsinki, and the protocols were validated by the Comité de Protection des Personnes Est IV. Sequence data were aligned to the reference genome GRCh37/hg19 with the use of the Burrows-Wheeler Aligner[13] and were processed with SAMtools.[14] We identified a heterozygous c.251A>G (p.Asp84Gly) missense mutation in *STIM1* (MIM 605921) (Table 1 and Figure 2). This mutation was present in all affected members and absent in the unaffected members, confirming autosomal-dominant inheritance. By Sanger sequencing of all *STIM1* coding exons and exon-intron boundaries in families with similar histological findings or by exome sequencing of two affected individuals from family 4, we found three additional *STIM1* heterozygous missense mutations segregating with the disease (Figure 2A). The mutations were numbered according to RefSeq accession number NM_003156.3 and GenBank accession number AAH21300.1, and none were listed in the SNP databases (dbSNP and 1000 Genomes) or in the National Heart, Lung, and Blood Institute (NHLBI) Exome Variant Server. The impact of variations were predicted with SIFT[15] and PolyPhen.[16] All four mutations, c.216C>G (p.His72Gln), c.251A>G (p.Asp84Gly), c.325C>A (p.His109Asn), and c.326A>G (p.His109Arg), cluster in the EF hands and affect highly conserved amino acids (Figures 2B and 2C). The resolved protein structure[2] revealed a close proximity of the affected residues (Figure 2D). The level of STIM1 was not decreased in myoblasts from individual II.1 in family 1 (Figure 2E).

Mutations in the EF hands are thought to disrupt Ca^{2+} binding and/or destabilize the interaction with the SAM domain,[17–19] unfold a hydrophobic cleft, and induce STIM1 oligomerization.[2] To assess the impact and the pathological significance of the identified mutations, we transfected C2C12 myoblasts with wild-type or altered STIM1 yellow-fluorescent-protein (YFP) constructs. Thapsigargin inhibits SERCA1 and induces SR Ca^{2+} depletion,

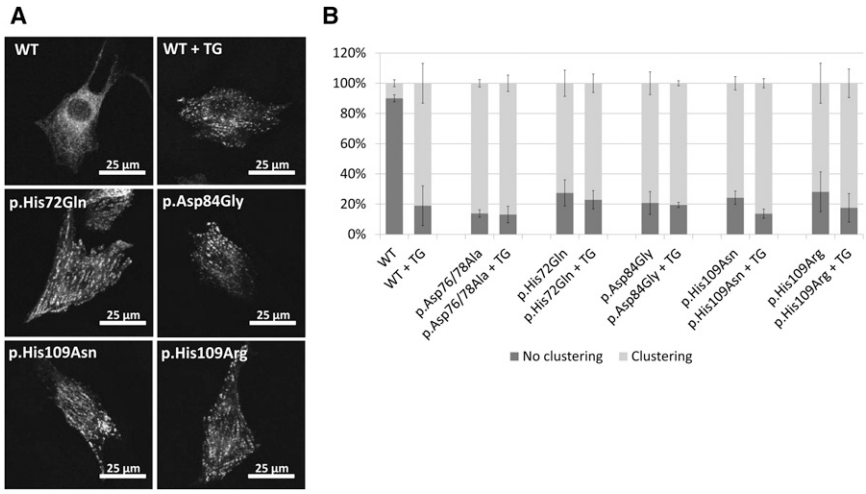

Figure 3. STIM1 Clustering in C2C12 Cells in Dependence of Thapsigargin and Quantification

(A) C2C12 myoblasts were transfected with wild-type or altered STIM1 YFP constructs with the use of Lipofectamine 2000 (Invitrogen, Carlsbad, CA, USA) and were incubated with or without thapsigargin (2 μM; Sigma-Aldrich, St. Louis, MO, USA). Point mutations c.216C>G (p.His72Gln), c.251A>G (p.Asp84Gly), c.325C>A (p.His109Asn), and c.326A>G (p.His109Arg) were introduced by site-directed mutagenesis with the *Pfu* DNA polymerase (Stratagene, La Jolla, CA, USA). Thapsigargin (TG) induced wild-type STIM1 oligomerization and clustering. A similar clustering was seen for all altered constructs independently of TG treatment. (B) Quantification of STIM1 YFP clustering in C2C12 cells in dependence of TG. At least 100 cells per transfection from three independent experiments were counted and assessed for STIM1 YFP clustering, i.e. for the presence of massive and area-wide clusters. The total number of counted cells was set to 100%, and the percentage of cells (*y* axis) containing clusters is shown as a light gray column. Error bars represent the SD. Wild-type STIM1 YFP barely clustered without TG addition. In contrast, all altered constructs showed massive clustering independently of TG. The human wild-type and p.Asp76/78Ala STIM1 YPF constructs were a kind gift from Nicolas Demaurex (University of Geneva, Switzerland). p.Asp76/78Ala is an artificial alteration reported to constitutively activate STIM1.

resulting in STIM1 clustering (Figure 3).[18] In contrast to the wild-type myoblasts, myoblasts transfected with any of the altered constructs displayed statistically significant STIM1 clustering independently of thapsigargin, indicating that Ca^{2+} sensing in the SR was impaired (Figures 3A and 3B). We confirmed this by monitoring the formation of STIM1 clusters in living cells by time-lapse microscopy (Movies S1 and S2). Similar results were obtained with a STIM1 construct harboring the artificial p.Asp76/78Ala (c.227A>C; c.233A>C) substitution reported to constitutively activate STIM1 (Figure S6).[19–21] These data demonstrate a strong impact of the mutations on STIM1 function by the triggering of STIM1 clustering independent of Ca^{2+}-store depletion.

We next investigated the pathological mechanism underlying the disease and monitored the Ca^{2+} response to SOCE in myoblasts established from an individual affected by the c.251A>G (p.Asp84Gly) mutation. Cells from individuals with other mutations were not available. Fluorescence-activated-cell-sorting analysis of myoblasts incubated with the Indo-1 Ca^{2+} indicator revealed a significantly higher basal cytoplasmic Ca^{2+} level in TAM cells than in control cells (Figure 4 and Table 2). We also measured a higher cytoplasmic Ca^{2+} influx in response to thapsigargin (2 μM) and subsequent addition of calcium (2 mM) to the medium in TAM cells. Accordingly, Ca^{2+} entry without thapsigargin treatment was also higher in TAM cells. We then challenged the mechanism regulating Ca^{2+} entry with a high extracellular Ca^{2+} concentration. Direct addition of 20 mM Ca^{2+} to cells in Ca^{2+}-free medium without prior Ca^{2+}-store depletion induced a massive Ca^{2+} influx in the TAM cells; in contrast, there was a low gradual increase in control cells. This constitutive activation of SOCE underlines a gain-of-function mechanism most likely resulting from the disruption of the Ca^{2+}-dependent inactivation of STIM1. The mutants appeared unable to sense the Ca^{2+} in the SR lumen and thereby oligomerized and clustered at the SR plasma-membrane junctions to constitutively activate CRACs. To assess the Ca^{2+} amount in the SR, we treated the myoblasts with 30 mM caffeine to induce extensive store depletion. Cytometric analysis showed that more Ca^{2+} was released from the SR in TAM cells than in control myoblasts (Figure S7), demonstrating an increased [Ca^{2+}] in both the SR and cytoplasm in TAM cells. It is possible that tubular aggregates directly arise from abnormal STIM1 clustering. Alternatively, an excess of intraluminal and/or cytosolic Ca^{2+}, as measured in TAM myoblasts, could promote SR-membrane remodeling in vivo.

STIM1 and *ORAI1* (MIM 610277) are highly expressed in skeletal muscle. They are both localized at the skeletal-muscle triad, a specialized junction between the ER and the plasma membrane, and mice deficient in STIM1 or ORAI1 display, among others, myopathic features.[17,22,23] Excessive store-operated Ca^{2+} influx, as in TAM myoblasts, has also been observed in myotubes from the mouse model[24,25] of Duchenne muscular dystrophy (DMD [MIM 310200]) and was sufficient to produce a muscular-dystrophy phenotype in mice.[26] It has furthermore been demonstrated for slow-channel congenital myasthenic syndrome (MIM 601462)—which involves the formation of tubular aggregates—that massive Ca^{2+} entry, due to abundant acetylcholine-receptor activity at the neuromuscular junction, damages the motor endplate and thereby induces the pathology.[27] These examples and our investigations suggest that altered Ca^{2+} homeostasis is implicated in skeletal-muscle dysfunction and that the augmented SOCE due to constitutively active STIM1 is

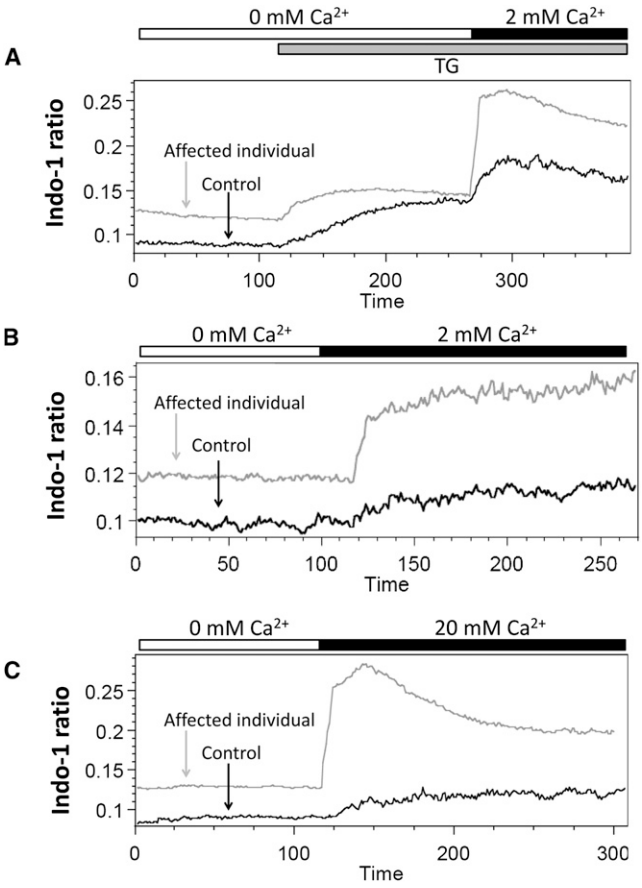

Figure 4. Impact of the STIM1 p.Asp84Gly Substitution on Ca^{2+} Homeostasis in TAM Myoblasts

Myoblasts (1.5×10^6 cells) were harvested and incubated in 1 ml medium containing Indo-1 (Invitrogen) and physiological Ca^{2+} concentrations and were then incubated in nominally Ca^{2+}-free Ringer solution. Data analysis was done with FlowJo software. Cell viability was verified by TO-PRO-3 staining (Invitrogen). The *y* axes show the Indo-1 ratio, and the *x* axes show the time in seconds.

(A) Cytometric analysis indicated a higher basal [Ca^{2+}] and an increased Ca^{2+} entry after store depletion with TG in myoblasts from individual II.1 (family 1, p.Asp84Gly).

(B) An increased Ca^{2+} influx in TAM cells was also seen without TG treatment.

(C) To challenge the mechanisms regulating Ca^{2+} influx, we directly added 20 mM Ca^{2+} without previous Ca^{2+}-store depletion, resulting in a significantly higher Ca^{2+} influx in the TAM myoblasts.

the major cause of the TAM phenotype. One of the hallmarks of DMD is the strongly elevated bloodstream CK level, which we also noted in all our TAM-affected families. Ca^{2+} is known to be implicated in membrane repair in skeletal muscle.[28] As a consequence of the constitutively active SOCE, cytosolic [Ca^{2+}] is steadily high, and defects in both SR structure and Ca^{2+} homeostasis might explain the muscle weakness and progressive course of TAM. Preventing excessive extracellular Ca^{2+} influx could therefore be a potential therapeutic approach for TAM.

Of note, a mouse line obtained by genome-wide random mutagenesis and harboring the same STIM1 p.Asp84Gly substitution as in one of our TAM-affected families displayed macrothrombocytopenia and an associated bleeding disorder, but skeletal muscle was not investigated.[29] Blood counts and coagulation tests of all our TAM-affected families were within normal ranges, and no families presented with a bleeding disorder (Table S3). In addition, recessive loss-of-function mutations in *STIM1* and *ORAI1* were previously reported in children with severe immune deficiency (MIM 612782 and MIM 612783). The affected individuals displayed additional neonatal hypotonia and type II fiber atrophy, and *Stim1*-knockout mice were reported to have perinatal muscle hypotrophy and lethality.[22,23,30,31] However, none of our TAM individuals had repetitive infections or hypotonia. Taken together, these findings emphasize the importance of STIM1 in blood platelets, T cell activation, and normal skeletal-muscle structure and function.

Acknowledgments

We thank the members of the families for their cooperation and interest in this study. We also thank Sophie Nicole, Danielle Chateau, Jean-Paul Leroy, Rana El Dahr, Nicolas Demaurex, Bernard Jost, Stéphanie Le Gras, Jean-Francois Pelissier, Sébastien Courrier, Valérie Biancalana, and Beate Heizmann for material supply, discussions, and technical assistance. This work was supported by grants from the Institut National de la Santé et de la Recherche Medicale, Centre National de la Recherche Scientifique, Université de Strasbourg, Aix-Marseille Université, Collège de France, Agence Nationale de la Recherche (ANR-11-BSV1-026), Fondation Maladies Rares, Groupement d'Intérêt Scientifique–Maladies Rares, Association Française contre les Myopathies, Muscular Dystrophy Association, and Myotubular Trust.

Table 2. Quantification of the Ca^{2+} Influx in Myoblasts from an Individual with TAM

Cell Line	Baseline	TG and 2 mM Ca^{2+}	2 mM Ca^{2+}	20 mM Ca^{2+}
Control 1	0.085 ± 0.005	0.063 ± 0.013	0.014 ± 0.005	0.052 ± 0.028
Control 2	0.079 ± 0.002	0.072 ± 0.019	0.031 ± 0.004	0.088 ± 0.009
Individual II.1 (family 1)	0.126 ± 0.007	0.108 ± 0.010	0.043 ± 0.006	0.125 ± 0.025
p value	2.95×10^{-13}	9.28×10^{-4}	1.34×10^{-2}	8.02×10^{-3}

Experiments were carried out with 1.5×10^6 cells and were repeated four times. The following abbreviation is used: TG, thapsigargin.

Web Resources

The URLs for data presented herein are as follows:

1000 Genomes, http://www.1000genomes.org/
dbSNP, http://www.ncbi.nlm.nih.gov/SNP/
FlowJo, http://www.treestar.com/
GenBank, http://www.ncbi.nlm.nih.gov/genbank/
NHLBI Exome Sequencing Project Exome Variant Server, http://evs.gs.washington.edu/EVS/
Online Mendelian Inheritance in Man (OMIM), http://www.omim.org/
PolyPhen, http://genetics.bwh.harvard.edu/pph/
RefSeq, http://www.ncbi.nlm.nih.gov/RefSeq
SIFT, http://sift.jcvi.org/

References

1. Li, Z., Lu, J., Xu, P., Xie, X., Chen, L., and Xu, T. (2007). Mapping the interacting domains of STIM1 and Orai1 in Ca2+ release-activated Ca2+ channel activation. J. Biol. Chem. *282*, 29448–29456.
2. Stathopulos, P.B., Zheng, L., Li, G.Y., Plevin, M.J., and Ikura, M. (2008). Structural and mechanistic insights into STIM1-mediated initiation of store-operated calcium entry. Cell *135*, 110–122.
3. Stathopulos, P.B., Li, G.Y., Plevin, M.J., Ames, J.B., and Ikura, M. (2006). Stored Ca2+ depletion-induced oligomerization of stromal interaction molecule 1 (STIM1) via the EF-SAM region: An initiation mechanism for capacitive Ca2+ entry. J. Biol. Chem. *281*, 35855–35862.
4. Luik, R.M., Wu, M.M., Buchanan, J., and Lewis, R.S. (2006). The elementary unit of store-operated Ca2+ entry: Local activation of CRAC channels by STIM1 at ER-plasma membrane junctions. J. Cell Biol. *174*, 815–825.
5. Park, C.Y., Hoover, P.J., Mullins, F.M., Bachhawat, P., Covington, E.D., Raunser, S., Walz, T., Garcia, K.C., Dolmetsch, R.E., and Lewis, R.S. (2009). STIM1 clusters and activates CRAC channels via direct binding of a cytosolic domain to Orai1. Cell *136*, 876–890.
6. Putney, J.W. (2010). Pharmacology of store-operated calcium channels. Mol. Interv. *10*, 209–218.
7. Wu, M.M., Buchanan, J., Luik, R.M., and Lewis, R.S. (2006). Ca2+ store depletion causes STIM1 to accumulate in ER regions closely associated with the plasma membrane. J. Cell Biol. *174*, 803–813.
8. Chevessier, F., Bauché-Godard, S., Leroy, J.P., Koenig, J., Paturneau-Jouas, M., Eymard, B., Hantaï, D., and Verdière-Sahuqué, M. (2005). The origin of tubular aggregates in human myopathies. J. Pathol. *207*, 313–323.
9. Boncompagni, S., Protasi, F., and Franzini-Armstrong, C. (2012). Sequential stages in the age-dependent gradual formation and accumulation of tubular aggregates in fast twitch muscle fibers: SERCA and calsequestrin involvement. Age (Dordr.) *34*, 27–41.
10. Engel, W.K., Bishop, D.W., and Cunningham, G.G. (1970). Tubular aggregates in type II muscle fibers: Ultrastructural and histochemical correlation. J. Ultrastruct. Res. *31*, 507–525.
11. Müller, H.D., Vielhaber, S., Brunn, A., and Schröder, J.M. (2001). Dominantly inherited myopathy with novel tubular aggregates containing 1-21 tubulofilamentous structures. Acta Neuropathol. *102*, 27–35.
12. Schiaffino, S. (2012). Tubular aggregates in skeletal muscle: Just a special type of protein aggregates? Neuromuscul. Disord. *22*, 199–207.
13. Li, H., and Durbin, R. (2009). Fast and accurate short read alignment with Burrows-Wheeler transform. Bioinformatics *25*, 1754–1760.
14. Li, H., Handsaker, B., Wysoker, A., Fennell, T., Ruan, J., Homer, N., Marth, G., Abecasis, G., and Durbin, R.; 1000 Genome Project Data Processing Subgroup. (2009). The Sequence Alignment/Map format and SAMtools. Bioinformatics *25*, 2078–2079.
15. Ng, P.C., and Henikoff, S. (2003). SIFT: Predicting amino acid changes that affect protein function. Nucleic Acids Res. *31*, 3812–3814.
16. Ramensky, V., Bork, P., and Sunyaev, S. (2002). Human non-synonymous SNPs: Server and survey. Nucleic Acids Res. *30*, 3894–3900.
17. Kiviluoto, S., Decuypere, J.P., De Smedt, H., Missiaen, L., Parys, J.B., and Bultynck, G. (2011). STIM1 as a key regulator for Ca2+ homeostasis in skeletal-muscle development and function. Skelet Muscle *1*, 16.
18. Liou, J., Kim, M.L., Heo, W.D., Jones, J.T., Myers, J.W., Ferrell, J.E., Jr., and Meyer, T. (2005). STIM is a Ca2+ sensor essential for Ca2+-store-depletion-triggered Ca2+ influx. Curr. Biol. *15*, 1235–1241.
19. Zhang, S.L., Yu, Y., Roos, J., Kozak, J.A., Deerinck, T.J., Ellisman, M.H., Stauderman, K.A., and Cahalan, M.D. (2005). STIM1 is a Ca2+ sensor that activates CRAC channels and migrates from the Ca2+ store to the plasma membrane. Nature *437*, 902–905.
20. Mercer, J.C., Dehaven, W.I., Smyth, J.T., Wedel, B., Boyles, R.R., Bird, G.S., and Putney, J.W., Jr. (2006). Large store-operated calcium selective currents due to co-expression of Orai1 or Orai2 with the intracellular calcium sensor, Stim1. J. Biol. Chem. *281*, 24979–24990.
21. Smyth, J.T., Dehaven, W.I., Bird, G.S., and Putney, J.W., Jr. (2008). Ca2+-store-dependent and -independent reversal of Stim1 localization and function. J. Cell Sci. *121*, 762–772.
22. McCarl, C.A., Picard, C., Khalil, S., Kawasaki, T., Röther, J., Papolos, A., Kutok, J., Hivroz, C., Ledeist, F., Plogmann, K., et al. (2009). ORAI1 deficiency and lack of store-operated Ca2+ entry cause immunodeficiency, myopathy, and ectodermal dysplasia. J. Allergy Clin. Immunol. *124*, 1311–1318, e7.
23. Stiber, J., Hawkins, A., Zhang, Z.S., Wang, S., Burch, J., Graham, V., Ward, C.C., Seth, M., Finch, E., Malouf, N., et al. (2008). STIM1 signalling controls store-operated calcium entry required for development and contractile function in skeletal muscle. Nat. Cell Biol. *10*, 688–697.
24. Boittin, F.X., Petermann, O., Hirn, C., Mittaud, P., Dorchies, O.M., Roulet, E., and Ruegg, U.T. (2006). Ca2+-independent phospholipase A2 enhances store-operated Ca2+ entry in dystrophic skeletal muscle fibers. J. Cell Sci. *119*, 3733–3742.
25. Edwards, J.N., Friedrich, O., Cully, T.R., von Wegner, F., Murphy, R.M., and Launikonis, B.S. (2010). Upregulation of

store-operated Ca2+ entry in dystrophic mdx mouse muscle. Am. J. Physiol. Cell Physiol. *299*, C42–C50.

26. Millay, D.P., Goonasekera, S.A., Sargent, M.A., Maillet, M., Aronow, B.J., and Molkentin, J.D. (2009). Calcium influx is sufficient to induce muscular dystrophy through a TRPC-dependent mechanism. Proc. Natl. Acad. Sci. USA *106*, 19023–19028.
27. Engel, A.G., Lambert, E.H., Mulder, D.M., Torres, C.F., Sahashi, K., Bertorini, T.E., and Whitaker, J.N. (1982). A newly recognized congenital myasthenic syndrome attributed to a prolonged open time of the acetylcholine-induced ion channel. Ann. Neurol. *11*, 553–569.
28. Idone, V., Tam, C., and Andrews, N.W. (2008). Two-way traffic on the road to plasma membrane repair. Trends Cell Biol. *18*, 552–559.
29. Grosse, J., Braun, A., Varga-Szabo, D., Beyersdorf, N., Schneider, B., Zeitlmann, L., Hanke, P., Schropp, P., Mühlstedt, S., Zorn, C., et al. (2007). An EF hand mutation in Stim1 causes premature platelet activation and bleeding in mice. J. Clin. Invest. *117*, 3540–3550.
30. Feske, S., Gwack, Y., Prakriya, M., Srikanth, S., Puppel, S.H., Tanasa, B., Hogan, P.G., Lewis, R.S., Daly, M., and Rao, A. (2006). A mutation in Orai1 causes immune deficiency by abrogating CRAC channel function. Nature *441*, 179–185.
31. Picard, C., McCarl, C.A., Papolos, A., Khalil, S., Lüthy, K., Hivroz, C., LeDeist, F., Rieux-Laucat, F., Rechavi, G., Rao, A., et al. (2009). STIM1 mutation associated with a syndrome of immunodeficiency and autoimmunity. N. Engl. J. Med. *360*, 1971–1980.